



Measured improvement of global magnetohydrodynamic mode stability at high-beta, and in reduced collisionality spherical torus plasma)

J. W. Berkery, S. A. Sabbagh, A. Balbaky, R. E. Bell, R. Betti, A. Diallo, S. P. Gerhardt, B. P. LeBlanc, J. Manickam, J. E. Menard, and M. Podestà

Citation: *Physics of Plasmas* (1994-present) **21**, 056112 (2014); doi: 10.1063/1.4876610

View online: <http://dx.doi.org/10.1063/1.4876610>

View Table of Contents: <http://scitation.aip.org/content/aip/journal/pop/21/5?ver=pdfcov>

Published by the [AIP Publishing](#)

Articles you may be interested in

[Suppressing electron turbulence and triggering internal transport barriers with reversed magnetic shear in the National Spherical Torus Experimenta\)](#)

Phys. Plasmas **19**, 056120 (2012); 10.1063/1.4718456

[Rotational stabilization of resistive wall modes in ITER advanced tokamak scenariosa\)](#)

Phys. Plasmas **17**, 056104 (2010); 10.1063/1.3318267

[Electron gyroscale fluctuation measurements in National Spherical Torus Experiment H-mode plasma\)](#)

Phys. Plasmas **16**, 112507 (2009); 10.1063/1.3262530

[Influence of global beta, shape, and rotation on the H-mode pedestal structure in DIII-Da\)](#)

Phys. Plasmas **15**, 056114 (2008); 10.1063/1.2894214

[Interpretation of core localized Alfvén eigenmodes in DIII-D and Joint European Torus reversed magnetic shear plasma\)](#)

Phys. Plasmas **13**, 056104 (2006); 10.1063/1.2186049



AIP | Journal of Applied Physics

Journal of Applied Physics is pleased to announce **André Anders** as its new Editor-in-Chief

Measured improvement of global magnetohydrodynamic mode stability at high-beta, and in reduced collisionality spherical torus plasmas^{a)}

J. W. Berkery,^{1,b)} S. A. Sabbagh,¹ A. Balbaky,¹ R. E. Bell,² R. Betti,³ A. Diallo,² S. P. Gerhardt,² B. P. LeBlanc,² J. Manickam,² J. E. Menard,² and M. Podestà²

¹Department of Applied Physics and Applied Mathematics, Columbia University, New York, New York 10027, USA

²Princeton Plasma Physics Laboratory, Princeton University, Princeton, New Jersey 08543, USA

³Laboratory for Laser Energetics, University of Rochester, Rochester, New York 14623, USA

(Received 23 January 2014; accepted 26 March 2014; published online 14 May 2014)

Global mode stability is studied in high- β National Spherical Torus Experiment (NSTX) plasmas to avoid disruptions. Dedicated experiments in NSTX using low frequency active magnetohydrodynamic spectroscopy of applied rotating $n=1$ magnetic fields revealed key dependencies of stability on plasma parameters. Observations from previous NSTX resistive wall mode (RWM) active control experiments and the wider NSTX disruption database indicated that the highest β_N plasmas were not the least stable. Significantly, here, stability was measured to increase at β_N/l_i higher than the point where disruptions were found. This favorable behavior is shown to correlate with kinetic stability rotational resonances, and an experimentally determined range of measured $E \times B$ frequency with improved stability is identified. Stable plasmas appear to benefit further from reduced collisionality, in agreement with expectation from kinetic RWM stabilization theory, but low collisionality plasmas are also susceptible to sudden instability when kinetic profiles change. © 2014 AIP Publishing LLC. [<http://dx.doi.org/10.1063/1.4876610>]

I. INTRODUCTION

Global magnetohydrodynamic (MHD) instabilities in magnetic fusion producing devices (such as the resistive wall mode (RWM)¹) are critically important to avoid or control as they lead to plasma disruption and potentially damaging electromagnetic forces and heat loads on the device structure. Plasma operation below marginal stability points is insufficient to ensure continuous operation in tokamaks, including ITER, because excursions from these conditions due to transients in plasma profiles can rapidly change a stable operational point to an unstable one. In addition, recent research has found that marginal stability conditions are not monotonic functions of important plasma parameters, such as the rotation profile² or collisionality.³

The National Spherical Torus Experiment (NSTX)⁴ has previously investigated passive stabilization⁵ and demonstrated active control⁶ of RWMs, accessing high normalized beta, $\beta_N = 7.4$ ($\beta_N \equiv 10^8 \langle \beta_i \rangle a B_0 / I_p$, ($\beta_i \equiv 2\mu_0 \langle p \rangle / B_0^2$), where $\langle p \rangle$ is the volume-average plasma pressure, B_0 is the magnetic field on axis, a is the minor radius, and I_p is the plasma current).⁷ In high β_N , low plasma internal inductance, l_i ($\beta_N/l_i > 11$) experiments in NSTX the probability of unstable RWMs causing a disruption was reduced from 48% to 14% with dual field component control.⁸ Here $l_i \equiv \langle B_p^2 \rangle / \langle B_p \rangle^2$ (where B_p is the poloidal magnetic field). Interestingly, disruptions due to RWMs occurred more frequently at intermediate values of β_N/l_i ,⁸ a trend reflected in the wider database of NSTX disruptions as well.⁹ Significantly, and for the first time, here stability was observed to *increase* at β_N/l_i higher

than the point where disruptions were found. The present work utilizes low frequency MHD spectroscopy measurements in this class of high β plasmas as a tool to provide a direct measurement of RWM stability.^{10,11} The dependencies of stability on collisionality and rotation are investigated and compared with theoretical expectations.³

II. MEASUREMENT OF GLOBAL MODE STABILITY

Dedicated experiments were performed in NSTX to measure the stability of long pulse, high β_N plasmas as a function of key plasma parameters for kinetic RWM stability, using low-frequency MHD spectroscopy. This is a natural extension of past experiments that directly accessed the RWM marginal stability point and found quantitative agreement to kinetic RWM stability theory.^{2,7} Here, low-frequency MHD spectroscopy is being performed on plasmas that access RWM marginal stability, with a small portion of these plasmas becoming unstable. In these cases, the mode amplitude grows on the RWM instability growth time, leading to plasma disruption.

Active MHD spectroscopy is an established experimental diagnostic technique¹² used to measure MHD mode stability when the plasma is stable^{10,13} by measuring the resonant field amplification (RFA)¹⁴ of a traveling toroidal mode number $n=1$ applied tracer field. The “low-frequency” version of this technique is used for studies of kink modes or RWMs, which have relatively slow growth rates. One could then apply a single-mode model to convert the measured RFA amplitude to a predicted RWM growth rate^{10,15,16} (or vice versa¹⁷). However, this is not necessary in order to demonstrate the change in stability with plasma parameters. Experimental evidence to date has shown that

^{a)}Paper T12 2, Bull. Am. Phys. Soc. **58**, 280 (2013).

^{b)}Invited speaker.

increasing amplitude generally indicates decreasing mode stability (although this is not necessarily the case depending on the structure of the applied vacuum magnetic field¹⁸). RFA amplitude, therefore, is a proxy for stability and a candidate real-time measurement for use in instability-avoidance feedback systems.¹⁹

Here, 40 Hz co-neutral beam injection (NBI) rotating $n = 1$ seed fields were applied with between 0.4 and 1 kA on the NSTX midplane RWM coils, and the $n = 1$ decomposition of the RFA on an array of 12 poloidal field sensors above the midplane ($B_p^u n = 1$) was measured. RFA amplitude is defined as the plasma response minus the vacuum response to the externally applied field, divided by the vacuum response, where each is measured at the upper sensor locations (superscript u): $|(B_{plasma}^u - B_{vac}^u)/B_{vac}^u|$. A series of 20 discharges with varying plasma current, toroidal field, and neutral beam heating power was generated in NSTX, which resulted in plasmas with $3.3 < \beta_N < 6.6$. The AC $n = 1$ fields did not significantly impact the plasma rotation, but each discharge was also subject to varying levels of non-resonant $n = 3$ magnetic braking²⁰ provided by the same coils, which provided controlled, steadily decreasing rotation to low levels.

Figure 1 shows a comparison of four of the discharges, showing $B_p^u n = 1$, β_N , carbon toroidal rotation at the plasma

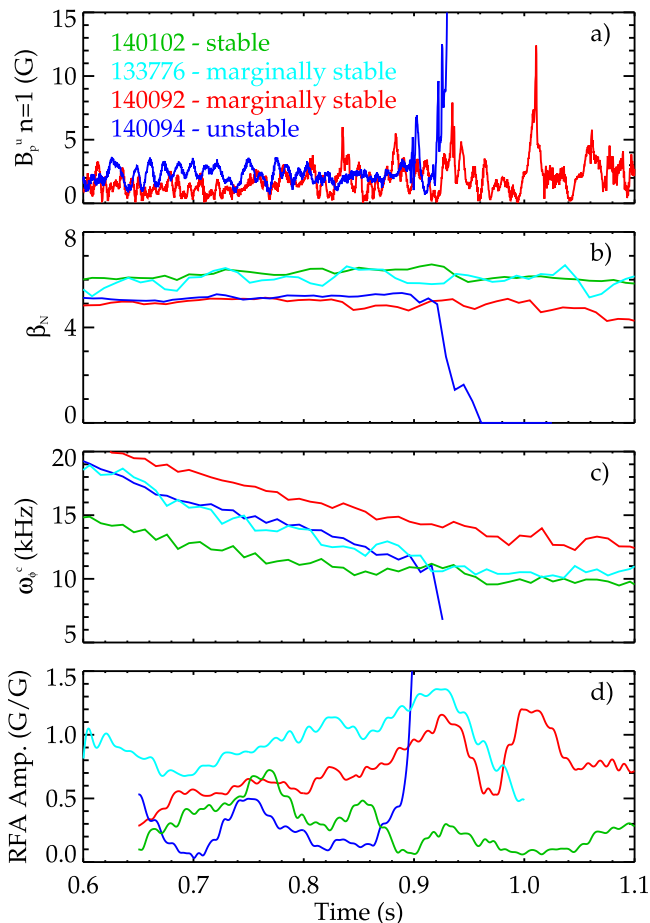


FIG. 1. Comparison of four NSTX discharges (two in (a)) showing: (a) $n = 1$ signal on the upper poloidal magnetic field sensors, (b) β_N , (c) carbon toroidal rotation near the core (CHERS channel 6), (d) $n = 1$ RFA amplitude vs. time.

core (charge-exchange recombination spectroscopy (CHERS) channel 6), ω_ϕ^c , and $n = 1$ RFA amplitude, vs. time. The noise level on the RFA amplitude measurement is approximately 0.1 G/G, as seen in Fig. 1(d). These cases illustrate the complexity of the dependence of the RWM marginal stability point on plasma rotation. The discharge shown by the blue trace goes unstable at 0.9 s when the plasma rotation reaches $\omega_\phi^c \sim 12$ kHz. The discharge shown in red has the same β_N , but has higher rotation and maintains stability, as might be expected from early RWM stabilization theory.¹ However, this discharge twice approaches marginal stability as indicated by increased $B_p^u n = 1$ and peaks in the RFA amplitude, but does not go unstable.

The discharges shown in cyan and green have higher β_N than the unstable (blue) discharge, and therefore would normally be thought to be less stable. The discharge shown in cyan does have elevated RFA amplitude, but maintains stability. Most surprisingly, the discharge shown in green has lower rotation but maintains stability with low RFA, which is counter-intuitive based on experiments²¹ and stability models yielding a simple critical rotation velocity for stability. In contrast, resonant kinetic RWM stabilization physics can explain this more complex behavior at low rotation.²

III. RWM STABILITY vs. β_N/l_i

Rather than attempting to fix all relevant plasma parameters but one in a data set (which is often difficult or impossible to accomplish in reality), here we take the approach of looking at the behavior of a restricted data set of stability measurements vs. individual plasma parameters and considering the general trends and the resulting stability boundaries. The discharges are restricted to those accessing among the highest β_N with boundary shapes and most plasma parameters held similar except for ω_ϕ , which was changed by magnetic braking, and collisionality, which was changed by varying the toroidal magnetic field and plasma current at constant safety factor.

Previous RFA studies,^{13,22} including in NSTX,¹¹ have shown that RFA amplitude generally increases with β_N . At near constant pressure peaking, which is the case for these high performance H-mode plasmas in NSTX, a more relevant parameter to measure global mode stability is β_N/l_i ,^{11,23} which accounts for decreased kink stability with broader current profiles (lower l_i). The RFA amplitude trajectories taken from the full database of twenty discharges, during time periods without rotating or locked tearing modes, show an increase to a broad peak near $\beta_N/l_i = 10$ (Fig. 2(a)). There is a large variation in RFA amplitude at a given β_N/l_i because other parameters, chiefly plasma rotation, are not constant. RFA amplitude then decreases at higher values of β_N/l_i , indicating increased mode stability. Examining some more specific examples, we see that the discharges shown in blue and green have the same β_N as those in red and cyan, respectively (Fig. 1(b)), but lower l_i , higher β_N/l_i (Fig. 2(a)), and lower RFA amplitude (Figs. 1(d) and 2).

Therefore, a significant result of the present work is that the global mode stability measured by MHD spectroscopy *increases* at the highest values of stability parameters in high

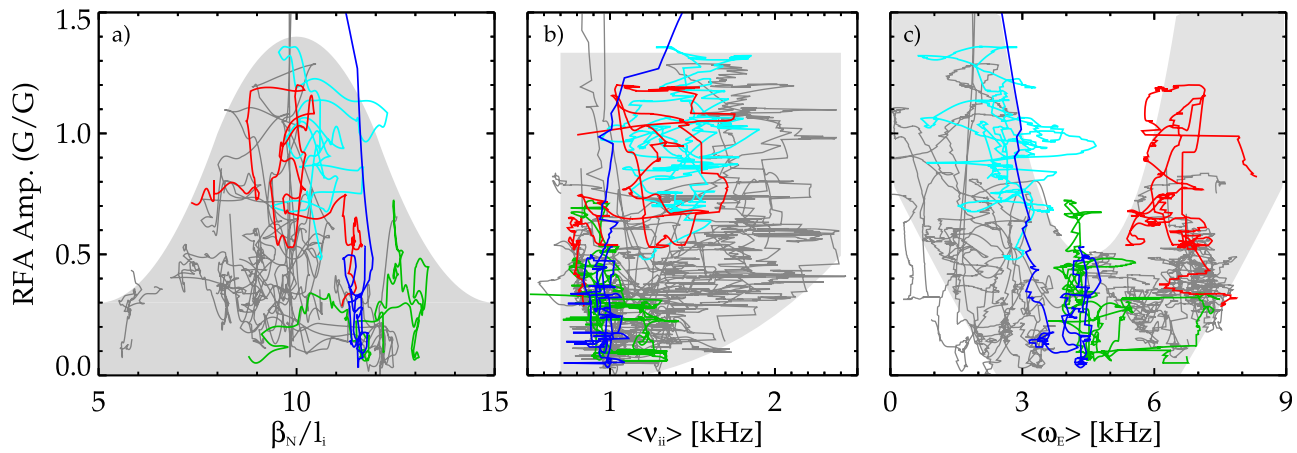


FIG. 2. RFA amplitude vs. (a) β_N/l_i , (b) an average ion-ion collision frequency, and (c) an average $E \times B$ frequency, $\langle \omega_E \rangle$. The colors are the same four discharges as in Fig. 1, with 16 other shots shown in grey. The grey backgrounds are meant as general guides to the trends in the data and the stability boundaries.

β_N NSTX plasmas, which is consistent with the observation of increased disruptivity at intermediate values of β_N/l_i in previous dedicated RWM control experiments⁸ and the wider disruption database⁹ in NSTX. Present analysis shows this result is not due to a second stability region for the RWM based on magnetic shear stabilization created by high pressure gradient^{24,25} but comes about because there is a correlation in these NSTX discharges between high β_N/l_i and rotational resonances that provide kinetic stabilization of the RWM,^{2,7} as will be demonstrated in this work. It should be noted that the possibility for kinetic effects to stabilize the mode more effectively near the high beta ideal MHD with-wall limit has been recognized theoretically.²⁶

IV. CONNECTION TO KINETIC RWM STABILITY PHYSICS THEORY

One important investigation is the effect of reduced collisionality on RWM stability. Figure 2(b) shows the evolution of the RFA amplitude over the discharge for the database of 20 NSTX shots, over which the average ion-ion collision frequency, $\langle \nu_{ii} \rangle$, is varied experimentally by a factor of 3.5. Here, $\langle \nu_{ii} \rangle$ is averaged over a poloidal flux range $\Psi_a/2 < \Psi < \Psi_p$ of the profile, where a is the plasma edge and p is the position of the density pedestal (the inflection point of a tanh fit to the density profile). Avoiding the outer flux region is necessary because rapidly decreasing density and temperature in that region cause large variation in evaluated quantities.

The experimental trend of stability as measured by RFA from the database of discharges does not show a strong scaling with collisionality in Fig. 2(b), but rather a general consistency with expectation from theory. Theory predicts that collisions have the competing effects of both dissipating mode energy and damping stabilizing kinetic effects.³ In the experiment, there is little change in RWM stability along the upper boundary of the data in Fig. 2(b) (marginally stable plasmas) indicated by the $n=1$ RFA amplitude between ~ 1.1 and 1.3 vs. $\langle \nu_{ii} \rangle$ between 0.8 and 2.4 kHz. In contrast, plasmas which have a stabilizing resonance between rotation and ion motion can in theory benefit from a reduction in collisionality, which allows those resonant effects to be

stronger.³ Correspondingly, as $\langle \nu_{ii} \rangle$ is reduced from 2.4 to 1.2 kHz, there is a clear decrease in RFA amplitude from 0.5 to 0 along the lower boundary where the plasma has greater stabilization by kinetic resonances.

Additionally, previous NSTX experimental research and kinetic theory have established the present understanding that a single point rotation measurement (as shown in Fig. 1(c)) is not sufficient as an indicator of RWM stability. Full kinetic RWM stability calculations with the MISK code^{2,27} capture the necessary physics and will be shown below. An intermediary step that can provide physical insight, however, is to examine the effect of plasma rotation in the context of kinetic resonances between the mode and the particles.

Kinetic resonances are stabilizing because when the trapped thermal ion's precession motion plus $E \times B$ motion around the torus is near zero in the frame of the slowly rotating mode ($|\omega_E - \omega_D| \approx 0$), energy is most efficiently transferred between the mode and the particles, reducing free energy driving the mode to grow.²⁶ This criterion is evaluated in a simple manner to determine if the result can be correlated to mode stability in a limited way. Figure 2(c) shows RFA amplitude plotted against $\langle \omega_E \rangle$, the $E \times B$ frequency averaged over the same Ψ range as $\langle \nu_{ii} \rangle$. The $E \times B$ frequency is related to the toroidal plasma rotation by $\omega_E \approx \omega_\phi + (1/en_i)(d(n_i T_i)/d\Psi)$, where n_i and T_i are the ion density and temperature. In the full kinetic treatment, the resonance criterion is considerably more complex (ω_D , for example, is dependent on particle pitch angle and energy).^{2,5} However, since ω_D is generally small (≈ 0), and ω_E decreases with Ψ , we can roughly project that a certain finite range of $\langle \omega_E \rangle$ inside the pedestal will provide a favorable resonance ($\omega_E \approx 0$) in the outer surfaces where the RWM eigenfunction is large. This could explain the low RFA amplitude in the 4 kHz $\langle \omega_E \rangle < 5$ kHz range in Fig. 2(c). Low rotation ($\omega_E < -\omega_D$) marginal stability (cyan) and instability (blue) appear below this. Intermediate rotation between resonances ($-\omega_D < \omega_E < \omega_b$, where ω_b is the bounce frequency) marginal stability (red) appears above, as predicted by kinetic stability theory.² In general in this set of NSTX discharges, there is a correlation between $\beta_N/l_i \sim 10$, the value which reaches the lowest stability as measured by

MHD spectroscopy, and off-resonant ω_E . Note that at higher rotation, stability should again increase due to bounce resonances, but this rotation range was not accessed in this experiment. We do not wish to imply that a “single point” rotation measurement (here actually an average ω_E over a range of Ψ) can generally be used as a reliable indicator of marginal stability. However, this simple criterion of an experimentally determined favorable $\langle\omega_E\rangle$ (≈ 4.5 kHz) could be used as a target for rotation profile control in future experiments to examine if plasma stability is increased by feedback toward this profile.

V. CALCULATION WITH THE MISK CODE

The preceding simple comparisons are insightful, but they neglect the more complex and complete physics included in the full MISK code^{2,27} calculation of kinetic stabilizing effects. The change in potential energy due to kinetic effects, δW_K , can be calculated with MISK for trapped thermal ions with a precession resonance only, δW_K (ion prec.), which is indicative of the strength of the precession resonance effect. In Fig. 3, the inverse of this quantity (normalized by the fluid no-wall δW) is shown (so that this plot can be directly compared to Fig. 2(a)) vs. β_N/l_i for 44 calculations from individual equilibria with $\beta_N/l_i \geq 10$ from the trajectories shown in Fig. 2(a). The calculations support the hypothesis that plasmas with β_N/l_i larger than ~ 10 , which are more stable in the experimental measurements, have generally larger precession resonance kinetic effects, whereas plasmas approaching β_N/l_i of 10 can have smaller kinetic effects and be less stable.

The MISK code can also be used to calculate an RWM growth rate normalized to the time constant of magnetic field penetration of the resistive wall, $\gamma\tau_w$, for greater insight on the dependence of the theoretical marginal

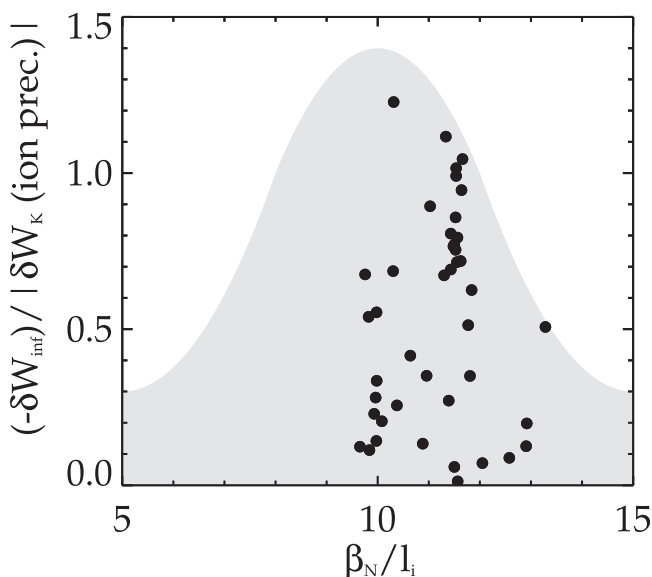


FIG. 3. The inverse of the ion precession drift resonance kinetic stabilization term, $(-\delta W_{\infty})/|\delta W_K(\text{ion prec.})|$, calculated by MISK vs. β_N/l_i in high β NSTX plasmas. The grey region corresponds to the operation space shown in Fig. 2(a).

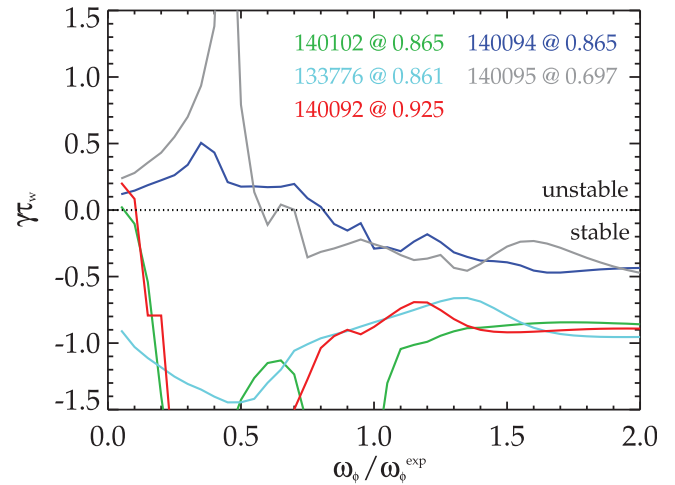


FIG. 4. MISK calculated $\gamma\tau_w$ vs. scaled experimental rotation. The colors are the same four discharges as in Figs. 1 and 2, with an additional shot shown in grey.

stability point vs. plasma parameters.^{2,3,5} Figure 4 shows the MISK-calculated $\gamma\tau_w$ (calculated using trapped and circulating thermal ions and electrons with precession and bounce or transit resonances) vs. rotation profiles that have been scaled from one-twentieth to twice the experimental profile, $\omega_{\phi}^{\text{exp}}$. Distinct experimental time points from the same four discharges as in Fig. 1 are used, with an additional equilibrium shown in grey (one of those in Fig. 2 with RFA amplitude > 1.5 , at a time just before this discharge goes unstable). The discharge shown in green has generally larger resonant kinetic effects and subsequently lower $\gamma\tau_w$ (high stability) which corresponds with low RFA amplitude (≈ 0.5). The time points selected for the discharges shown in red and cyan are for when each has an RFA amplitude of roughly one. Correspondingly, MISK finds these discharges to be stable, but with a growth rate slightly closer to marginal. Finally, MISK finds that the two equilibria shown in blue and grey are marginally stable and predicts that with slightly decreased rotation these discharges will go unstable.

The prediction of instability with a 20% reduced rotation profile for the discharge shown in blue agrees quite favorably with what actually happens in the experiment as the plasma slows from ~ 12 kHz to ~ 10 kHz in the core from the time of the equilibrium evaluated here at 0.865 s to the time of instability at ~ 0.9 s (see Fig. 1(c)). To put this in context, the error in the MISK calculations may be characterized as follows. For the blue trace in Fig. 4 with the experimental rotation profile ($\omega_{\phi}/\omega_{\phi}^{\text{exp}} = 1$), the growth rate was found to be $\gamma\tau_w = -0.29 \pm 0.015$ when random Gaussian measurement errors (in rotation frequency, and ion and electron density and temperature) were propagated through the code and the standard deviation of 20 otherwise identical code runs was taken. Additionally the deviation of the trends of the discharges shown in blue and grey from $0.5 < \omega_{\phi}/\omega_{\phi}^{\text{exp}} < 1.5$ from smooth curve fits is about ± 0.05 . Finally, sensitivities to code assumptions and settings have been previously found to give changes in $\gamma\tau_w$ of less than ± 0.1 .² The kinetic stabilization physics in MISK will continue to be compared to

marginally stable equilibria to improve what is already close quantitative agreement with the marginal stability point.

VI. DISCUSSION

Stability measurements using MHD spectroscopy of (mostly) stable NSTX plasmas have illuminated the roles of collisionality, rotation, and β_N/l_i in RWM stability and have added support to the theory of RWM stabilization through kinetic resonances. RFA amplitude increases for plasmas with ω_E above and below the range of precession drift resonance (Fig. 2(b)). An important difference from previous experiments on DIII-D that used the MHD spectroscopy technique^{10,13,15–17,19} is that here the MHD spectroscopy is being performed on plasmas that reach RWM marginal stability, with a small portion of these plasmas becoming unstable. Stability is weakest, and unstable plasmas are found, at intermediate β_N/l_i values (Fig. 2(a)) due to a correlation with off-resonant ω_E . Stability *increases* at the highest β_N/l_i .

Attention is now turning to practical application of the knowledge gained by kinetic stability physics insight, calculations, and comparisons with experiment, to use in a disruption avoidance algorithm in NSTX-Upgrade. NSTX-U is projected to operate in a similar range of β_N/l_i to that shown here while potentially having considerably lower collisionality and better control over the rotation magnitude and profile (both from the new, more tangential neutral beam and from improved rotation profile control capabilities).²⁸ Additionally, RWM stability has been identified as critical for high performance NSTX-U operation.²⁸

In future machines, the quantity $\langle\omega_E\rangle$ could conceivably be monitored by a real-time charge exchange recombination spectroscopy system that measures ion rotation, density, and temperature profiles ($\omega_E \approx \omega_\phi + (1/en_i)(d(n_i T_i)/d\Psi)$). Realistically, however, future devices may only have real-time measurements of ω_ϕ^c at limited radial locations, such as is planned for NSTX-U,²⁹ in which case $\langle\omega_E\rangle$ could still be modeled in real time with modeled density and temperature profiles. A system monitoring real-time measurements of plasma rotation and RFA amplitude (similar to Figs. 1(c) and 1(d)) and modeled $\langle\omega_E\rangle$ (Fig. 2(c)) could be quite useful to detect steady, relatively slow approaches toward marginal stability. Then various actuators such as non-resonant magnetic braking²⁰ or changing neutral beam injection sources for rotation control could be used to return the plasma to a more stable state.

At low collisionality, however, the plasma stability gradient is expected to increase as a function of rotation,³ so the plasma can change between a stable and unstable state quite quickly (~ 10 ms time scale) as rotation is changed. Combined with frequency limitations on real-time RFA measurements (40 Hz here, for example), this calls into question a strategy of relying solely on real-time RFA feedback for disruption avoidance in future machines. This emphasizes the need for rotation profile control independent of RFA feedback and informed by kinetic stability theory and for active (magnetic) RWM control when either slow, controlled or sudden, uncontrolled changes take the plasma through a marginal stability point.

ACKNOWLEDGMENTS

This research was supported by the U.S. Department of Energy under Contract Nos. DE-FG02-99ER54524 and DE-AC02-09CH11466.

- ¹A. Bondeson and D. J. Ward, *Phys. Rev. Lett.* **72**, 2709 (1994).
- ²J. Berkery, S. Sabbagh, R. Betti, B. Hu, R. Bell, S. Gerhardt, J. Manickam, and K. Tritz, *Phys. Rev. Lett.* **104**, 035003 (2010).
- ³J. Berkery, S. A. Sabbagh, R. Betti, R. E. Bell, S. P. Gerhardt, B. P. LeBlanc, and H. Yuh, *Phys. Rev. Lett.* **106**, 075004 (2011).
- ⁴M. Ono, S. Kaye, Y. Peng, G. Barnes, W. Blanchard, M. Carter, J. Chrzanowski, L. Dudek, R. Ewig, D. Gates, R. Hatcher, T. Jarboe, S. Jardin, D. Johnson, R. Kaita, M. Kalish, C. Kessel, H. Kugel, R. Maingi, R. Majeski, J. Manickam, B. McCormack, J. Menard, D. Mueller, B. Nelson, B. Nelson, C. Neumeyer, G. Oliaro, F. Paoletti, R. Parsells, E. Perry, N. Pomphrey, S. Ramakrishnan, R. Raman, G. Rewoldt, J. Robinson, A. Roquemore, P. Ryan, S. Sabbagh, D. Swain, E. Synakowski, M. Viola, M. Williams, and J. Wilson, *Nucl. Fusion* **40**, 557 (2000).
- ⁵J. W. Berkery, S. A. Sabbagh, H. Reimerdes, R. Betti, B. Hu, R. Bell, S. P. Gerhardt, J. Manickam, and M. Podestà, *Phys. Plasmas* **17**, 082504 (2010).
- ⁶S. Sabbagh, R. E. Bell, J. E. Menard, D. A. Gates, A. C. Sontag, J. M. Bialek, B. P. LeBlanc, F. M. Levinton, K. Tritz, and H. Yuh, *Phys. Rev. Lett.* **97**, 045004 (2006).
- ⁷S. A. Sabbagh, J. W. Berkery, R. E. Bell, J. M. Bialek, S. P. Gerhardt, J. E. Menard, R. Betti, D. A. Gates, B. Hu, O. Katsuro-Hopkins, B. P. LeBlanc, F. Levinton, J. Manickam, K. Tritz, and H. Yuh, *Nucl. Fusion* **50**, 025020 (2010).
- ⁸S. A. Sabbagh and NSTX Team, *Nucl. Fusion* **53**, 104007 (2013).
- ⁹S. P. Gerhardt, R. E. Bell, A. Diallo, D. Gates, B. P. LeBlanc, J. E. Menard, D. Mueller, S. A. Sabbagh, V. Soukhanovskii, K. Tritz, and H. Yuh, *Nucl. Fusion* **53**, 043020 (2013).
- ¹⁰H. Reimerdes, M. S. Chu, A. M. Garafalo, G. L. Jackson, R. J. La Haye, G. Navratil, M. Okabayashi, J. T. Scoville, and E. J. Strait, *Phys. Rev. Lett.* **93**, 135002 (2004).
- ¹¹S. A. Sabbagh, A. C. Sontag, J. M. Bialek, D. A. Gates, A. H. Glasser, J. E. Menard, W. Zhu, M. G. Bell, R. E. Bell, A. Bondeson, C. E. Bush, J. D. Callen, M. S. Chu, C. C. Hegna, S. M. Kaye, L. L. Lao, B. P. LeBlanc, Y. Q. Liu, R. Maingi, D. Mueller, K. C. Shaing, D. Stutman, K. Tritz, and C. Zhang, *Nucl. Fusion* **46**, 635 (2006).
- ¹²A. Fasoli, D. Borba, G. Bosia, D. J. Campbell, J. A. Dobbins, C. Gormezano, J. Jacquinet, P. Lavanchy, J. B. Lister, P. Marmillod, J.-M. Moret, A. Santagiustina, and S. Sharapov, *Phys. Rev. Lett.* **75**, 645 (1995).
- ¹³A. Garofalo, T. H. Jensen, and E. J. Strait, *Phys. Plasmas* **10**, 4776 (2003).
- ¹⁴A. H. Boozer, *Phys. Rev. Lett.* **86**, 5059 (2001).
- ¹⁵H. Reimerdes, J. Bialek, M. S. Chance, M. S. Chu, A. M. Garofalo, P. Gohil, Y. In, G. L. Jackson, R. J. Jayakumar, T. H. Jensen, J. S. Kim, R. J. La Haye, Y. Q. Liu, J. E. Menard, G. A. Navratil, M. Okabayashi, J. T. Scoville, E. J. Strait, D. D. Szymanski, and H. Takahashi, *Nucl. Fusion* **45**, 368 (2005).
- ¹⁶H. Reimerdes, A. M. Garofalo, M. Okabayashi, E. J. Strait, R. Betti, M. S. Chu, B. Hu, Y. In, G. L. Jackson, R. La Haye, M. Lanctot, Y. Liu, G. Navratil, W. Solomon, H. Takahashi, R. Groebner, and DIII-D Team, *Plasma Phys. Controlled Fusion* **49**, B349 (2007).
- ¹⁷H. Reimerdes, J. W. Berkery, M. J. Lanctot, A. M. Garofalo, J. M. Hanson, Y. In, M. Okabayashi, S. A. Sabbagh, and E. J. Strait, *Phys. Rev. Lett.* **106**, 215002 (2011).
- ¹⁸M. J. Lanctot, H. Reimerdes, A. M. Garofalo, M. S. Chu, J. M. Hanson, Y. Q. Liu, G. A. Navratil, I. N. Bogatu, Y. In, G. L. Jackson, R. J. La Haye, M. Okabayashi, J.-K. Park, M. J. Schaffer, O. Schmitz, E. J. Strait, and A. D. Turnbull, *Phys. Plasmas* **18**, 056121 (2011).
- ¹⁹J. Hanson, H. Reimerdes, M. J. Lanctot, Y. In, R. J. La Haye, G. L. Jackson, G. A. Navratil, M. Okabayashi, P. E. Sieck, and E. J. Strait, *Nucl. Fusion* **52**, 013003 (2012).
- ²⁰W. Zhu, S. A. Sabbagh, R. E. Bell, M. G. Bell, B. P. LeBlanc, S. M. Kaye, F. M. Levinton, J. E. Menard, K. C. Shaing, A. C. Sontag, and H. Yuh, *Phys. Rev. Lett.* **96**, 225002 (2006).
- ²¹E. Strait, A. M. Garofalo, M. E. Austin, J. Bialek, M. S. Chu, E. D. Fredrickson, L. L. Lao, R. J. La Haye, E. A. Lazarus, G. McKee, G. A. Navratil, M. Okabayashi, B. W. Rice, S. A. Sabbagh, J. T. Scoville, T. S. Taylor, A. D. Turnbull, M. L. Walker, and DIII-D Team, *Nucl. Fusion* **39**, 1977 (1999).

- ²²I. Chapman, C. G. Gimblett, M. P. Gryaznevich, T. C. Hender, D. F. Howell, Y. Q. Liu, and S. D. Pinches, *Plasma Phys. Controlled Fusion* **53**, 065022 (2011).
- ²³W. Howl, A. D. Turnbull, T. S. Taylor, L. L. Lao, F. J. Helton, J. R. Ferron, and E. J. Strait, *Phys. Fluids B* **4**, 1724 (1992).
- ²⁴J. Greene and M. Chance, *Nucl. Fusion* **21**, 453 (1981).
- ²⁵S. Sabbagh, M. H. Hughes, M. W. Phillips, A. M. M. Todd, and G. A. Navratil, *Nucl. Fusion* **29**, 423 (1989).
- ²⁶B. Hu and R. Betti, *Phys. Rev. Lett.* **93**, 105002 (2004).
- ²⁷B. Hu, R. Betti, and J. Manickam, *Phys. Plasmas* **12**, 057301 (2005).
- ²⁸S. P. Gerhardt, R. Andre, and J. E. Menard, *Nucl. Fusion* **52**, 083020 (2012).
- ²⁹M. Podestà and R. Bell, *Rev. Sci. Instrum.* **83**, 033503 (2012).